Research Article | Vol. 24, No. 20 | 3 Oct 2016 | OPTICS EXPRESS 22635

Optics EXPRESS

Novel approximation of misalignment fading modeled by Beckmann distribution on free-space optical links

RUBÉN BOLUDA-RUIZ,[1,*] ANTONIO GARCÍA-ZAMBRANA,[1] CARMEN CASTILLO-VÁZQUEZ,[2] AND BEATRIZ CASTILLO-VÁZQUEZ[1]

[1] *Department of Communications Engineering, University of Málaga, E-29071 Málaga, Spain*
[2] *Department of Mathematical Analysis, Statistics and Operations Research and Applied Mathematics, University of Málaga, E-29071 Málaga, Spain*
[*] *rbr@ic.uma.es*

Abstract: A novel accurate and useful approximation of the well-known Beckmann distribution is presented here, which is used to model generalized pointing errors in the context of free-space optical (FSO) communication systems. We derive an approximate closed-form probability density function (PDF) for the composite gamma-gamma (GG) atmospheric turbulence with the pointing error model using the proposed approximation of the Beckmann distribution, which is valid for most practical terrestrial FSO links. This approximation takes into account the effect of the beam width, different jitters for the elevation and the horizontal displacement and the simultaneous effect of nonzero boresight errors for each axis at the receiver plane. Additionally, the proposed approximation allows us to delimit two different FSO scenarios. The first of them is when atmospheric turbulence is the dominant effect in relation to generalized pointing errors, and the second one when generalized pointing error is the dominant effect in relation to atmospheric turbulence. The second FSO scenario has not been studied in-depth by the research community. Moreover, the accuracy of the method is measured both visually and quantitatively using curve-fitting metrics. Simulation results are further included to confirm the analytical results.

OCIS codes: (010.1330) Atmospheric turbulence; (060.2605) Free-space optical communication; (060.4510) Optical communications.

References and links

1. M. A. Khalighi and M. Uysal, "Survey on free space optical communication: A communication theory perspective," Communications Surveys and Tutorials, IEEE **16**(4), 2231–2258 (2014).
2. I. I. Kim, R. Stieger, J. A. Koontz, C. Moursund, M. Barclay, P. Adhikari, J. Schuster, E. Korevaar, R. Ruigrok, and C. DeCusatis, "Wireless optical transmission of fast ethernet, FDDI, ATM, and ESCON protocol data using the TerraLink laser communication system," Opt. Eng. **37**(12), 3143–3155 (1998).
3. L. C. Andrews, R. L. Phillips, and C. Hopen, *Laser Beam Scintillation with Applications*, vol. 99 (SPIE, 2001).
4. M. A. Al-Habash, L. C. Andrews, and R. L. Phillips, "Mathematical model for the irradiance probability density function of a laser beam propagating through turbulent media," Opt. Eng. **40**, 8 (2001).
5. L. C. Andrews and R. L. Phillips, *Laser Beam Propagation through Random Media*, vol. 1 (SPIE, 2005).
6. S. Arnon, "Effects of atmospheric turbulence and building sway on optical wireless-communication systems," Opt. Lett. **28**(2), 129–131 (2003).
7. A. K. Majumdar and J. C. Ricklin, *Free-space Laser Communications: Principles and Advances*, vol. 2 (Springer Science and Business Media, 2010).
8. D. K. Borah and D. G. Voelz, "Pointing error effects on free-space optical communication links in the presence of atmospheric turbulence," J. Lightwave Technol. **27**(18), 3965–3973 (2009).
9. A. A. Farid and S. Hranilovic, "Outage capacity optimization for free-space optical links with pointing errors," J. Lightwave Technol. **25**(7), 1702–1710 (2007).
10. W. Gappmair, S. Hranilovic, and E. Leitgeb, "OOK performance for terrestrial FSO links in turbulent atmosphere with pointing errors modeled by Hoyt distributions," IEEE Commun. Lett. **15**(8), 875–877 (2011).
11. F. Yang, J. Cheng, and T. Tsiftsis, "Free-space optical communication with nonzero boresight pointing errors," IEEE Trans. Commun. **62**(2), 713–725 (2014).
12. M. K. Simon and M.-S. Alouini, *Digital Communications over Fading Channels*, 2nd ed. (Wiley, 2005).
13. H. AlQuwaiee, H. C. Yang, and M. Alouini, "On the asymptotic capacity of dual-aperture FSO systems with a generalized pointing error model," IEEE Transactions on Wireless Commun. **99**, 1 (2016).

#267467 http://dx.doi.org/10.1364/OE.24.022635
Journal © 2016 Received 31 May 2016; revised 12 Sep 2016; accepted 14 Sep 2016; published 21 Sep 2016

Optics EXPRESS

14. I. I. Kim, B. McArthur, and E. J. Korevaar, "Comparison of laser beam propagation at 785 nm and 1550 nm in fog and haze for optical wireless communications," in *Information Technologies 2000*, pp. 26–37 (International Society for Optics and Photonics, 2001).
15. I. S. Gradshteyn and I. M. Ryzhik, *Table of Integrals, Series and Products*, 7th ed. (Academic Inc., 2007).
16. N. Wang and J. Cheng, "Moment-based estimation for the shape parameters of the gamma-gamma atmospheric turbulence model," Opt. Express **18**(12), 12,824–12,831 (2010).
17. A. García-Zambrana, B. Castillo-Vázquez, and C. Castillo-Vázquez, "Asymptotic error-rate analysis of FSO links using transmit laser selection over gamma-gamma atmospheric turbulence channels with pointing errors," Opt. Express **19**(24), 2096–2109 (2011).
18. A. García-Zambrana, R. Boluda-Ruiz, C. Castillo-Vázquez, and B. Castillo-Vázquez, "Novel space-time trellis codes for free-space optical communications using transmit laser selection," Opt. Express **23**(19), 24195–24211 (2015).
19. R. Boluda-Ruiz, A. García-Zambrana, B. Castillo-Vázquez, and C. Castillo-Vázquez, "MISO Relay-Assisted FSO Systems Over Gamma-Gamma Fading Channels With Pointing Errors," IEEE Photonics Technol. Lett. **28**(3), 229–232 (2016).
20. R. Boluda-Ruiz, A. García-Zambrana, B. Castillo-Vázquez, and C. Castillo-Vázquez, "Impact of nonzero boresight pointing error on ergodic capacity of MIMO FSO communication systems," Opt. Express **24**(4), 3513–3534 (2016).
21. S. C. Schwartz and Y.-S. Yeh, "On the Distribution Function and Moments of Power Sums With Log-Normal Components," Bell System Technical Journal **61**(7), 1441–1462 (1982).
22. H. G. Sandalidis, T. A. Tsiftsis, and G. K. Karagiannidis, "Optical wireless communications with heterodyne detection over turbulence channels with pointing errors," J. Lightwave Technol. **27**(20), 4440–4445 (2009).
23. Wolfram Research, Inc., "The Wolfram functions site," URL http://functions.wolfram.com.
24. Z. Wang and G. B. Giannakis, "A simple and general parameterization quantifying performance in fading channels," IEEE Trans. Commun. **51**(8), 1389–1398 (2003).
25. A. P. Prudnikov, Y. A. Brychkov, and O. I. Marichev, *Integrals and series Volume 2: Special Functions*, vol. 2, 1st ed. (Gordon and Breach Science Publishers, 1986).
26. S. Bloom, E. Korevaar, J. Schuster, and H. Willebrand, "Understanding the performance of free-space optics," J. Opt. Netw. **2**(6), 178–200 (2003).
27. N. B. Mehta, J. Wu, A. F. Molisch, and J. Zhang, "Approximating a sum of random variables with a lognormal," IEEE Trans. Wireless Commun. **6**(7), 2690–2699 (2007).

1. Introduction

Free-space optical (FSO) communication systems have confirmed to be a strong alternative to radio-frequency (RF) systems due to inherent advantages including a huge license free-spectrum, immunity to RF interferences and high security. This exciting technology is able to transmit high-bandwidth data through the atmosphere when fiber optic systems are neither practical nor feasible [1]. This kind of systems are able to provide high speed links in the range of 1-8 km [2]. However, there are a variety of deleterious features of the atmospheric channel that might lead to serious signal fading, and even the complete loss of signal altogether. Atmospheric turbulence results in fluctuations in both the intensity and the phase of the received signal, severely degrading the link performance [3]. Some statistical models have been presented to describe and examine such fluctuations in intensity and phase from weak to strong turbulence, for instance, gamma-gamma (GG) distribution has gained a wide acceptance for moderate-to-strong turbulence regime [4, 5]. In addition to the effect of the atmospheric turbulence, FSO communication links are strongly affected by pointing errors, resulting in serious misalignment of fixed-position laser communication systems. Building sway due to wind loads, differential heating and cooling, or ground motion over time can result in an important misalignment error [6, 7]. Additionally, pointing errors can also arise due to mechanical misalignment, errors in tracking systems, or due to mechanical vibrations present in the FSO system [8]. At the same time, physical obstructions such as birds, tree limbs, or other factors can temporarily or permanently block the laser line-of-sight.

Over the past decade, there have been some authors that have proposed several statistical models for studying the impact of pointing errors on FSO communication systems [9–11]. In [9], a pointing error model was proposed, where the effect of beam width, detector size and independent identical Gaussian distributions for the elevation and the horizontal displacement were considered. This model continues using in a great deal of research articles due to its

Optics EXPRESS

simplicity from a mathematical point of view, where the radial displacement at the receiver is determined by a Rayleigh distribution, as well as due to its realistic approach. In [10], the analysis carried out in [9] was extended in order to assume different jitters for the elevation and the horizontal displacement, i.e., the radial displacement at the receiver follows a Hoyt distribution. In [11], a pointing error model once again based on [9] was proposed considering a nonzero boresight error at the receiver for independent identical Gaussian distributions for the elevation and the horizontal displacement, i.e, the radial displacement at the receiver follows a lognormal-Rician distribution. Unlike satellite FSO communication systems, where is generally accepted to assume the same jitter variance for the elevation and the horizontal displacement, as assumed in [11], a more realistic approach was assumed in [10] for terrestrial FSO links since physical impacts such as dynamic wind loads, thermal expansion and weak earthquakes have different impact on horizontal and vertical axes of constructions. It is evident that there is quite an important need for considering a much more realistic pointing error model, where the effect of different jitters for the elevation and the horizontal displacement as well as a nonzero boresight error at the receiver are assumed. In that model, the radial displacement at the receiver is determined by the Beckmann distribution [12], which is a versatile statistical model that includes many distributions as special cases such as Rayleigh, Hoyt and lognormal-Rician, among others. This generalized approach for studying pointing errors was considered recently in [13] for evaluating the asymptotic ergodic capacity of FSO links over log-normal (LN) and GG atmospheric turbulence channels. It must be noted that neither a closed-form expression nor an approximate expression for the composite probability density function (PDF) with atmospheric turbulence and pointing errors were obtained.

In the present work we perform a deep analysis of the performance of FSO links, which are modeled by GG atmospheric turbulence with generalized pointing errors. The misalignment between transmitter and receiver follows a Beckmann distribution, whose integral-form PDF is unknown. To the best of our knowledge, finding a closed-form expression of the combined PDF of GG atmospheric turbulence and generalized pointing errors might be mathematically intractable. Motivated by the above, we introduce an efficient and accurate approximation of the Beckmann distribution in this work, which is used to model generalized pointing errors with quite high precision. In this way, we derive an approximate closed-form PDF for the composite GG atmospheric turbulence with the pointing error model using the proposed approximation of the Beckmann distribution, which is valid for typical values in terrestrial FSO links as well as for more extreme FSO scenarios. The performance of FSO communication links is analyzed in terms of the outage probability (OP) and bit-error rate (BER). An asymptotic BER analysis is also included in order to study how the diversity order gain and coding gain are affected by generalized pointing errors. Moreover, the accuracy of the method is measured both visually and quantitatively using curve-fitting metrics. Numerical evaluation for a range of valid parameters shows good accuracy for moderate jitters, i.e., for most practical FSO applications.

2. System model

Here, we adopt a single-input/single-output (SISO) FSO link with one transmitter or laser source and one receive aperture. The use of infrared technologies based on intensity-modulation and direct-detection (IM/DD) is assumed due to their simplicity and low cost. The intensity of the emitted light is used to transmit the information, and the photodetector directly detects changes in the light intensity without the need for a local oscillator. The received electrical signal for a SISO FSO link is given by

$$Y = \eta X I_T + Z, \tag{1}$$

where η is the detector responsivity, assumed hereinafter to be the unity, X is the transmitted optical power, I_T is the equivalent real-value fading gain of the channel between the source and the receiver, and Z is additive white Gaussian noise (AWGN) with zero mean and variance

Optics EXPRESS

$\sigma^2 = N_0/2$, i.e. $Z \sim N(0, N_0/2)$, independent of the on/off state of the received bit. The irradiance is considered to be a product of three factors, i.e. $I_T = L \cdot I_a \cdot I_p$, atmospheric path loss L, atmospheric turbulence I_a, and geometric spread and pointing errors I_p. The atmospheric path loss L is determined by the exponential Beers-Lambert law as $L = e^{-\Phi d_{SD}}$, where d_{SD} is the link distance and Φ is the atmospheric attenuation coefficient. The Φ parameter is given by $\Phi = (3.91/V(km))\,(\lambda(nm)/550)^{-q}$, where V is the visibility in kilometers, λ is the wavelength in nanometers and q is the size distribution of the scattering particles, being $q = 1.3$ for clear visibility (6 km $< V <$ 50 km), and $q = 0.16V + 0.34$ for haze visibility (1 km $< V <$ 6 km) [14]. Note that both atmospheric turbulence and pointing errors are considered to be statistically independent.

3. FSO channel fading model

3.1. Atmospheric turbulence model

The atmospheric turbulence is modeled by the GG distribution in order to consider a wide range of turbulence conditions (moderate-to-strong) [3, 4], whose PDF is given by

$$f_{I_a}(i) = \frac{2(\alpha\beta)^{(\alpha+\beta)/2}}{\Gamma(\alpha)\Gamma(\beta)} i^{((\alpha+\beta)/2)-1} K_{\alpha-\beta}\left(2\sqrt{\alpha\beta i}\right), \quad i \geq 0 \tag{2}$$

where $\Gamma(\cdot)$ is the well-known Gamma function and $K_\nu(\cdot)$ is the νth-order modified Bessel function of the second kind [15]. The parameters related to atmospheric turbulence, α and β, can be selected to achieve a good agreement between Eq. (2) and measurement data [4]. Alternatively, assuming negligible inner scale, α and β can directly be linked to physical parameters through the following expressions [4, 16]:

$$\alpha = \left[\exp\left(0.49\sigma_R^2/(1 + 1.11\sigma_R^{12/5})^{7/6}\right) - 1\right]^{-1}, \tag{3a}$$

$$\beta = \left[\exp\left(0.51\sigma_R^2/(1 + 0.69\sigma_R^{12/5})^{5/6}\right) - 1\right]^{-1}, \tag{3b}$$

where $\sigma_R^2 = 1.23\kappa^{7/6} C_n^2 d_{SD}^{11/6}$ is the Rytov variance for a plane wave, which is a measure of the optical turbulence strength. Here, $\kappa = 2\pi/\lambda$ is the optical wave number, λ is the wavelength, d_{SD} is the source-destination link distance, and C_n^2 is the refractive index structure parameter, which is the most significant parameter that determines the turbulence strength. Clearly, C_n^2 not only depends on the altitude, but also on the local conditions such as terrain type, geographic location, cloud cover, and time of day [7]. The C_n^2 parameter is typically within the range 10^{-13}-10^{-17} $m^{-2/3}$ [3]. It must be emphasized that α and β cannot arbitrarily be chosen in FSO applications due to the fact that both parameters are related to the Rytov variance. In this fashion, it can be shown that the relationship $\alpha > \beta$ always holds, and the β parameter is lower bounded above 1 as the Rytov variance approaches ∞ [16]. It must be noted that the value of the Rytov variance can also be used to characterize different turbulence levels: weak-turbulence refers to $\sigma_R^2 \leq 0.3$, moderate-turbulence has $0.3 < \sigma_R^2 \leq 5$ and strong-turbulence corresponds to $\sigma_R^2 > 5$ [16].

3.2. A generalized pointing error model

With regard to the impact of generalized pointing errors, we use a model of generalized misalignment fading, where the effect of beam width, detector size, different jitters for the elevation and the horizontal displacement and the effect of nonzero boresight error are considered. The attenuation due to geometric spread and pointing errors can be approximated, as in [9], by

$$I_p(r; z) \approx A_0 \exp\left(-\frac{2r^2}{\omega_{zeq}^2}\right), \quad r \geq 0, \tag{4}$$

Optics EXPRESS

where $v = \sqrt{\pi}a/\sqrt{2}\omega_z$, $A_0 = [\mathrm{erf}(v)]^2$ is the fraction of the collected power at $r = 0$, and $\omega_{z_{eq}}^2 = \omega_z^2\sqrt{\pi}\mathrm{erf}(v)/2v\exp(-v^2)$ is the equivalent beam width. The beam width ω_z can be approximated by $\omega_z = \theta z$, where θ is the transmit divergence angle describing the increase in beam radius with distance from the transmitter. We can express the radial displacement r at the receiver plane as $r^2 = x^2 + y^2$, where x and y represent the horizontal displacement and the elevation, respectively. Both x and y are modeled as independent Gaussian random variables with different jitters for the horizontal displacement (σ_x) and the elevation (σ_y), and different boresight errors in each axis of the receiver plane ($s^2 = \mu_x^2 + \mu_y^2$), i.e., $x \sim N(\mu_x, \sigma_x)$ and $y \sim N(\mu_y, \sigma_y)$. It must be noted that a circular detection aperture of radius a is assumed at the receiver, as shown in Fig. 1, where the beam footprint with generalized misalignment on the detector plane is illustrated. Furthermore, the approximation in Eq. (4) is in good agreement with the exact value when the normalized beam width $\omega_z/a > 6$. Let us define a couple of useful

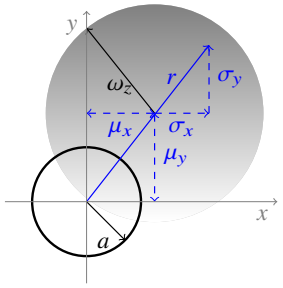

Fig. 1. Beam footprint with generalized pointing errors on the receiver aperture plane.

pointing error parameters such as $\varphi_x = \omega_{z_{eq}}/2\sigma_x$ and $\varphi_y = \omega_{z_{eq}}/2\sigma_y$. These parameters are the ratios between the equivalent beam radius at the receiver and the corresponding pointing error displacement standard deviation (jitter) at the receiver.

As can be deduced from the previous paragraph, the radial displacement r at the receiver is distributed according to the well-known Beckmann distribution, whose integral-form PDF can be found in [12] as follows

$$f_r(r) = \frac{r}{2\pi\sigma_x\sigma_y}\int_0^{2\pi}\exp\left(-\frac{(r\cos\theta-\mu_x)^2}{2\sigma_x^2} - \frac{\left(r\sin\theta-\mu_y\right)^2}{2\sigma_y^2}\right)d\theta, \quad r \geq 0. \tag{5}$$

On the one hand, it must be mentioned that finding the combined effect of the atmospheric turbulence and generalized pointing errors might be mathematically intractable due to the fact that the Beckmann distribution presents certain impediments from a practical point of view since a closed-form solution for its integral in Eq. (5) is unknown. On the other hand, there are no published studies that investigate the effect of generalized pointing errors following a Beckamn distribution and, hence, there is clearly a need for researching on this topic. In this way, a novel approximation of the Beckmann distribution is presented here, which is only valid for evaluating the performance of FSO links, in order to find an approximate PDF that allows us to obtain its asymptotic behavior and delimit two different FSO scenarios. The first of them is when atmospheric turbulence is the dominant effect in relation to generalized pointing errors, and the second one when generalized pointing error is the dominant effect in relation to the atmospheric turbulence. Unfortunately, delimiting these two FSO scenarios has not been analyzed in-depth in the literature when the radial displacement r is not determined by a Rayleigh distribution, as in [10, 11]. In [10], obtained expressions for the BER over GG fading channels when the radial displacement r is determined by a Hoyt distribution are not valid for larger amounts of misalignment, i.e. when pointing error becomes dominant in relation to atmospheric turbulence

Optics EXPRESS

and, hence, not knowing when pointing errors begin to be dominant. At the same time, in [11], the derived diversity order gain is given as a function of the atmospheric turbulence parameters, not being valid the obtained asymptotic expressions for the BER over GG fading channels when pointing error is the dominant effect, and, hence, as in [10], not knowing when pointing errors begin to be dominant.

3.3. A novel approximation of the Beckmann distribution

Now, a novel approximation of the Beckmann distribution is presented and analyzed. As a result, the PDF in Eq. (5), i.e. the Beckmann distribution, is approximated by a modified Rayleigh distribution of σ_{mod} parameter. The advantage of approximating the Beckmann distribution by a modified Rayleigh distribution is twofold. First, when the radial displacement r at the receiver is determined by a Rayleigh distribution, the corresponding PDF of I_p can easily be obtained as in [9]. Second, the combined effect of GG atmospheric turbulence and pointing errors based on a modified Rayleigh distribution allows us to asymptotically analyze the performance of FSO communication systems and, hence, studying how basic parameters impact on the FSO systems as well as optimizing some of them such as beam width for potential FSO applications. Quite interesting conclusions have been drawn from the asymptotic behavior in different FSO topics such as multiple-input/multiple-output (MIMO) FSO systems, cooperative FSO systems, space-time codes, among others [17–20].

For convenience, let us consider $u = r^2$ and, hence, it can be demonstrated that the squared radial displacement r^2 follows a exponential distribution when r follows a modified Rayleigh distribution, given by

$$f_{r^2}(u) = \frac{1}{2\sigma_{\text{mod}}^2} \exp\left(-\frac{u}{2\sigma_{\text{mod}}^2}\right), \quad u \geq 0. \tag{6}$$

The σ_{mod} parameter is used to estimate the diversity order gain when the pointing error is the dominant effect in relation to the atmospheric turbulence as well as to delimit the two FSO scenarios previously commented. By using the method of central moments, we can obtain the expression of the σ_{mod} parameter from the third-order central moment. This method is quite simple and yields consistent estimators under not very strong assumptions. We observed through numerical observations that the diversity order gain when the pointing error is the dominant effect can accurately be approximated from the third-order central moment, not deriving a relevant improvement for higher-order central moments. The main idea is to balance between the third-order central moment corresponding to the squared radial displacement (r follows a Beckmann distribution) and the third-order central moment corresponding to the exponential distribution given in Eq. (6). A central moment can be defined as the expected value of a specified integer power of the deviation of the random variable from the mean and is defined as $\Omega_n^{\chi} = \mathbb{E}[(\chi - \mathbb{E}[\chi])^n]$ with $\mathbb{E}[\cdot]$ denoting expectation. Hence, the third-order central moment corresponding to the squared radial displacement, where r follows a Beckmann distribution, can easily be expressed from the third-order central moment corresponding to the distribution of the sum of two squared normal random variates, obtaining

$$\Omega_3^{r^2} = 8\sigma_x^4\left(3\mu_x^2 + \sigma_x^2\right) + 8\sigma_y^4\left(3\mu_y^2 + \sigma_y^2\right), \tag{7}$$

and the third-order central moment corresponding to the exponential distribution is derived as

$$\Omega_3^{u} = 16\sigma_{\text{mod}}^6. \tag{8}$$

Now, matching Eq. (7) and Eq. (8), we can derive the corresponding expression of the σ_{mod}^2 parameter, which can readily be expressed as follows

$$\sigma_{\text{mod}}^2 = \left(\frac{3\mu_x^2\sigma_x^4 + 3\mu_y^2\sigma_y^4 + \sigma_x^6 + \sigma_y^6}{2}\right)^{1/3}. \tag{9}$$

Optics EXPRESS

As can be observed in Eq. (9), this expression reduces to the simplest case, i.e., the Rayleigh distribution, when a zero boresight error is considered as well as same jitters. Finally, the Beckmann distribution can accurately be approximated by a modified Rayleigh distribution as follows

$$f_r(r) \simeq \frac{r}{\sigma_{\text{mod}}^2} \exp\left(-\frac{r^2}{2\sigma_{\text{mod}}^2}\right), \quad r \geq 0. \tag{10}$$

Similar to [9], combining Eq. (4) and Eq. (10), the PDF corresponding to I_p is approximated by

$$f_{I_p}(i) \simeq \frac{\varphi_{\text{mod}}^2}{(A_0 G)^{\varphi_{\text{mod}}^2}} i^{\varphi_{\text{mod}}^2 - 1}, \quad 0 \leq i \leq A_0 G \tag{11}$$

where $\varphi_{\text{mod}} = \omega_{z_{eq}}/2\sigma_{\text{mod}}$. We have derived an approximation of the PDF corresponding to the random variable I_p, whose radial displacement r follows a Beckmann distribution of four parameters: μ_x, μ_y, σ_x and σ_y, by a PDF whose radial displacement r follows a modified Rayleigh distribution of one parameter: σ_{mod}. As can be deduced from Eq. (6), only one degree of freedom can be used to estimate the PDF of I_p. This degree of freedom has been used to balance the third-order central moment, which have a strong impact on the obtained diversity order gain when the pointing error is the dominant effect in relation to the atmospheric turbulence. At the same time, to balance the mismatch between expectations, a new G parameter is added to the PDF in Eq. (11) to get a better fit.

Next, this G parameter is derived as follows. Taking as reference the method published in [21] for approximating the log-normal variates sum by Schwartz and Yeh, which is quite accurate for estimating the CDF for small values of its argument, we match the moment in the log-domain, i.e., it equates the first moment or expectation of $\ln(I_p)$ when r is determined by a Beckmann distribution with $\ln(I_p)$ when r is determined by a modified Rayleigh distribution. Knowing that I_p is approximated as in Eq. (4), the logarithm of I_p can be expressed as $\ln(I_p) = \ln(A_0) - 2r^2/\omega_{z_{eq}}^2$. Hence, the expectation of $\ln(I_p)$ is given by

$$\mathbb{E}[\ln(I_p)] = \ln(A_0) - (2/\omega_{z_{eq}}^2)\mathbb{E}[r^2]. \tag{12}$$

In this way, the expectation of $\ln(I_p)$ when r is determined by a Beckmann distribution is easily obtained from the moment generating function (MGF) corresponding to the squared Beckmann distribution r^2. This MGF can be found in [12]. Hence, making use of that MGF, we can compute the expectation of $\ln(I_p)$ when r is determined by a Beckmann distribution as follows

$$\mathbb{E}[\ln(I_p)] = \ln(A_0) - 2(\mu_x^2 + \mu_y^2 + \sigma_x^2 + \sigma_y^2)/\omega_{z_{eq}}^2. \tag{13}$$

Therefore, the expectation of $\ln(I_p)$ when r is determined by a modified Rayleigh distribution is easily obtained as

$$\mathbb{E}[\ln(I_p)] = \ln(A_0) + \ln(G) - 1/\varphi_{\text{mod}}^2. \tag{14}$$

Now, matching Eq. (13) and Eq. (14), we derive the corresponding expression of G as

$$G = \exp\left(\frac{1}{\varphi_{\text{mod}}^2} - \frac{1}{2\varphi_x^2} - \frac{1}{2\varphi_y^2} - \frac{\mu_x^2}{2\sigma_x^2\varphi_x^2} - \frac{\mu_y^2}{2\sigma_y^2\varphi_y^2}\right). \tag{15}$$

Note that a new A_{mod} parameter is defined as $A_{\text{mod}} = A_0 G$.

3.4. Combined effect of atmospheric turbulence and generalized pointing errors

Using the previous PDFs for atmospheric turbulence and misalignment fading, a closed-form expression of the combined PDF of I_T was derived in [22] when the radial displacement r

Optics EXPRESS

is determined by a Rayleigh distribution. Therefore, that expression can be used to compute the combined effect of the GG atmospheric turbulence and generalized pointing errors in this work but substituting the corresponding parameters A_0 and φ^2 by the corresponding parameters derived in the previous subsection A_{mod} and φ^2_{mod} as

$$f_{I_T}(i) \simeq \frac{\alpha\beta\varphi^2_{\text{mod}} i^{-1}}{A_{\text{mod}} L\Gamma(\alpha)\Gamma(\beta)} G^{3,0}_{1,3}\left(\frac{\alpha\beta}{A_{\text{mod}} L} i \,\middle|\, \begin{matrix} \varphi^2_{\text{mod}}+1 \\ \varphi^2_{\text{mod}}, \alpha, \beta \end{matrix}\right), \quad i \geq 0, \tag{16}$$

where $G^{m,n}_{p,q}[\cdot]$ is the Meijer's G-function [15]. The corresponding cumulative distribution function (CDF) is derived using [23] as

$$F_{I_T}(i) \simeq \frac{\varphi^2_{\text{mod}}}{\Gamma(\alpha)\Gamma(\beta)} G^{3,1}_{2,4}\left(\frac{\alpha\beta}{A_{\text{mod}} L} i \,\middle|\, \begin{matrix} 1, \varphi^2_{\text{mod}}+1 \\ \varphi^2_{\text{mod}}, \alpha, \beta, 0 \end{matrix}\right). \quad i \geq 0. \tag{17}$$

As commented before, the PDF in Eq. (16) is approximated by a single polynomial term as $f_{I_T}(i) \approx a_T i^{b_T-1}$, based on the fact that the asymptotic behavior of the system performance is dominated by the behavior of the PDF near the origin, i.e. $f_{I_T}(i)$ at $i \to 0$ determines high SNR performance [24]. Hence, using the series expansion corresponding to the Meijer's G-function [23], we can obtain the following asymptotic expression for the PDF in Eq. (16) as

$$f_{I_T}(i) \approx a_T i^{b_T-1} = \begin{cases} \frac{\varphi^2_{\text{mod}}(\alpha\beta)^{\beta}\Gamma(\alpha-\beta)}{(A_{\text{mod}} L)^{\beta}\Gamma(\alpha)\Gamma(\beta)\left(\varphi^2_{\text{mod}}-\beta\right)} i^{\beta-1}, & \varphi^2_{\text{mod}} > \beta \\ \frac{\varphi^2_{\text{mod}}(\alpha\beta)^{\varphi^2_{\text{mod}}}\Gamma\left(\alpha-\varphi^2_{\text{mod}}\right)\Gamma\left(\beta-\varphi^2_{\text{mod}}\right)}{(A_{\text{mod}} L)^{\varphi^2_{\text{mod}}}\Gamma(\alpha)\Gamma(\beta)} i^{\varphi^2_{\text{mod}}-1}. & \varphi^2_{\text{mod}} < \beta \end{cases} \tag{18}$$

Note that different expressions for a_T and b_T are derived in Eq. (18) depending on the relation between φ^2_{mod} and β.

4. Performance analysis of FSO links with generalized pointing errors

4.1. Outage performance analysis

Now, outage performance over GG atmospheric channels with generalized pointing errors is analyzed. Outage probability, P_{out}, can be defined as the probability that the instantaneous combined SNR, γ_T, falls below a certain specified threshold, γ_{th}, which is a protection value of the SNR above which the quality of the channel is satisfactory as

$$P_{\text{out}} := P(\gamma_T \leq \gamma_{th}) = \int_0^{\gamma_{th}} f_{\gamma_T}(i) di. \tag{19}$$

The received electrical SNR can be defined as $\gamma_T = 4\gamma i^2$, where $\gamma = P^2_{\text{opt}} T_b / N_0$ represents the normalized received electrical SNR in absence of turbulence, P_{opt} is the average optical power and T_b is the bit period. Using Eq. (19), the outage probability can be written as

$$P_{\text{out}} = P(4\gamma i^2 \leq \gamma_{th}) = \int_0^{\sqrt{\gamma_{th}/4\gamma}} f_{I_T}(i) di = F_{I_T}\left(\sqrt{\frac{\gamma_{th}}{4\gamma}}\right). \tag{20}$$

4.2. Asymptotic bit-error rate performance analysis

In this section, we obtain an asymptotic closed-form expression in order to quantify the bit error probability for this SISO FSO communications system at high SNR, taking advantage of the simpler expression in Eq. (18). The asymptotic performance is characterized by two parameters: the diversity order (G_d) and coding (G_c) gains. In this way, the conditional BER for the considered SISO FSO system assuming channel state information (CSI) at the receiver

Optics EXPRESS

is given by $P_b(I_T) = Q\left(\sqrt{4P_{opt}^2 T_b/2N_0 i}\right)$, where $Q(\cdot)$ is the Gaussian-Q function. Hence, the average BER, P_b, can be obtained by averaging $P_b(I_T)$ over the PDF as follows

$$P_b = \int_0^\infty Q\left(\sqrt{2\gamma\xi i}\right) f_{I_T}(i)di. \tag{21}$$

In order to evaluate the integral in Eq. (21), we can use that the Q-function is related to the complementary error function $\mathrm{erfc}(\cdot)$ by $\mathrm{erfc}(x) = 2Q(\sqrt{2}x)$ [15] and the fact that $\int_0^\infty \mathrm{erfc}(cx)x^{\alpha-1}e^{-px}dx$ can be found in [25], obtaining an asymptotic closed-form solution for FSO links with generalized pointing errors as follows

$$P_b \doteq \frac{a_T\Gamma((b_T+1)/2)}{2b_T\sqrt{\pi}}\gamma^{-b_T/2}. \tag{22}$$

It must be noted that the average BER behaves asymptotically as $(G_c\gamma)^{-G_d}$. At high SNR, the diversity order gain determines the slope of the BER versus average SNR curve in a log-log scale and the coding gain (in decibels) determines the shift of the curve in SNR.

5. Numerical results

In this section, the proposed approximation for modeling the effect of generalized pointing errors on FSO links is evaluated over different atmospheric turbulence conditions and different misalignment error values. Note that the system configuration adopted in this work is used in most practical terrestrial FSO systems as in [2, 9, 11, 26], but also more extreme FSO scenarios are analyzed. Different weather conditions are adopted: haze visibility of 4 km with $C_n^2 = 1.7 \times 10^{-14}\ m^{-2/3}$ and clear visibility of 16 km with $C_n^2 = 8 \times 10^{-14}\ m^{-2/3}$, corresponding to moderate and strong turbulence conditions, respectively. A source-destination link distance of $d_{SD} = 3$ km is assumed together with a value of wavelength of $\lambda = 1550$ nm. Here, α and β are calculated from Eq. (3) for GG atmospheric turbulence. Pointing errors are present here assuming normalized beam width values of $\omega_z/a = \{7, 10\}$ as well as different normalized jitter values and nonzero boresight errors.

Firstly, the results corresponding to the outage performance analysis given in Section 4.1 are illustrated in Fig. 2(a) for moderate turbulence and Fig. 2(b) for strong turbulence as a function of the inverse normalized threshold SNR, γ/γ_{th}. Analogously, the results corresponding to the asymptotic BER performance analysis given in Section 4.2 are illustrated in Fig. 3(a) for moderate turbulence and Fig. 3(b) for strong turbulence, assuming the same FSO scenario as in Fig. 2. Different normalized jitter values for the elevation and horizontal displacement as well as different normalized nonzero boresight errors for each axes are assumed in Figs. 2 and 3 in order to carefully analyze how terrestrial FSO links are affected by generalized pointing errors. Taking into account the proposed approximation in this work, two different FSO scenarios are analyzed depending on the relationship $\beta < \varphi_{\mathrm{mod}}^2$ is satisfied or not. In this way, when this condition is satisfied, different normalized jitter values of $(\sigma_x/a, \sigma_y/a) = \{(2,1), (3,2), (4,3)\}$ together with normalized boresight error values of $(\mu_x/a, \mu_y/a) = (1,2)$ are considered in Figs. 2(a) and 3(a) for moderate turbulence conditions. Based on this, a higher diversity order, which is determined by the β parameter, is achieved when atmospheric turbulence is the dominant effect. In other words, the diversity order only depends on atmospheric turbulence, while the coding gain is affected by the degradation effect induced by generalized pointing errors. Analogously, different normalized jitter values of $(\sigma_x/a, \sigma_y/a) = \{(1, 0.1), (2,1), (3,2)\}$ together with normalized boresight error values of $(\mu_x/a, \mu_y/a) = (3,1)$ are considered in Figs. 2(b) and 3(b) for strong turbulence conditions. These results are quite similar to those commented previously so that same conclusions can be drawn. At the same time, the performance is also evaluated for larger amounts of generalized misalignment, showing that the proposed approximation is in good

Optics EXPRESS

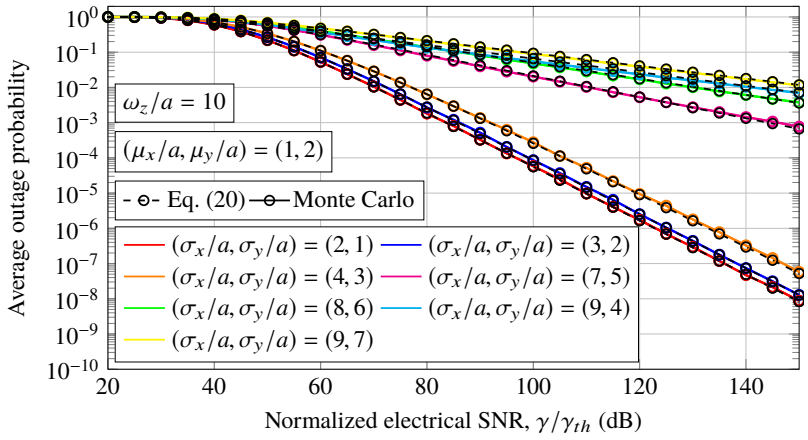

(a) Moderate turbulence.

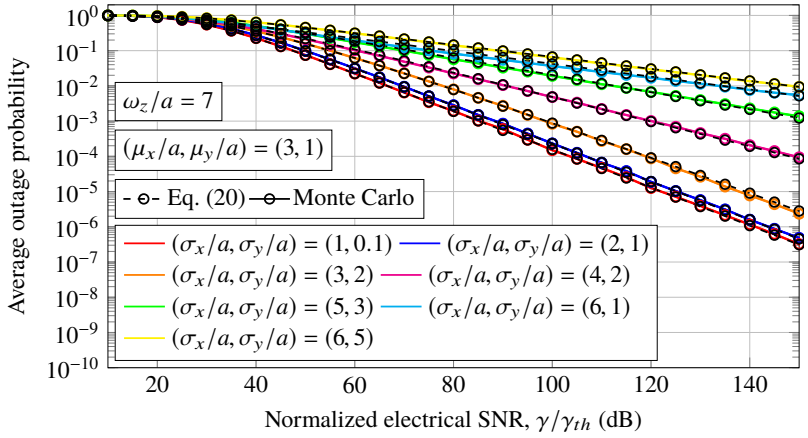

(b) Strong turbulence.

Fig. 2. Outage performance over GG atmospheric turbulence and generalized misalignment fading channels, when different weather conditions (a) $C_n^2 = 1.7 \times 10^{-14}\ m^{-2/3}$ and (b) $C_n^2 = 8 \times 10^{-14}\ m^{-2/3}$ are assumed for a link distance of $d_{SD} = 3$ km.

agreement with extreme FSO scenarios, i.e., when atmospheric turbulence is not the dominant effect. In other words, when the condition $\beta < \varphi^2_{\text{mod}}$ is not satisfied and, hence, the diversity order is determined by φ^2_{mod}, which depends on the normalized beam width, normalized jitters and normalized boresight errors. As expected, the obtained performance in both outage probability and BER is notably decreased as a result of assuming much more severe pointing errors, such as normalized jitter values of $(\sigma_x/a, \sigma_y/a) = \{(7, 5), (8, 6), (9, 4), (9, 7)\}$ together with normalized boresight error values of $(\mu_x/a, \mu_y/a) = (1, 2)$ for moderate turbulence in Figs. 2(a) and 3(a), and normalized jitter values of $(\sigma_x/a, \sigma_y/a) = \{(4, 2), (5, 3), (6, 1), (6, 5)\}$ together with normalized boresight error values of $(\mu_x/a, \mu_y/a) = (3, 1)$ for strong turbulence in Figs. 2(b) and 3(b). In order to confirm the accuracy and usefulness of the proposed approximation, Monte Carlo simulation results, where the FSO link is modeled by using the statistical model given in Eq. (1), are furthermore included by using solid line generating the corresponding variates from the exact combined PDF.

Due to the long simulation time involved, simulation results only up to 10^{-9} are included in

Optics EXPRESS

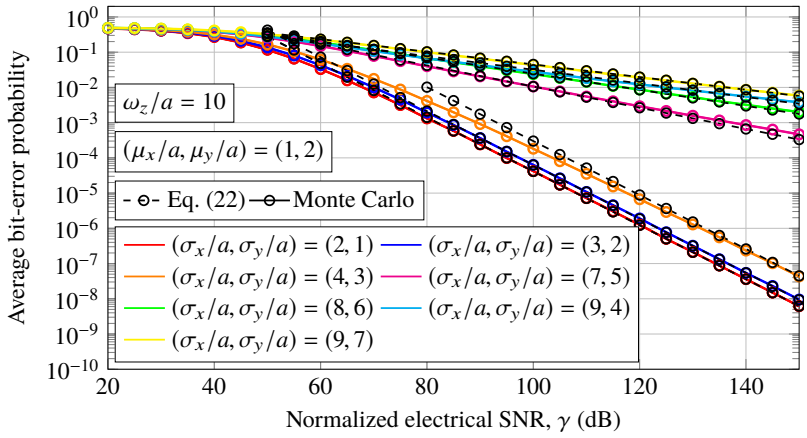

(a) Moderate turbulence.

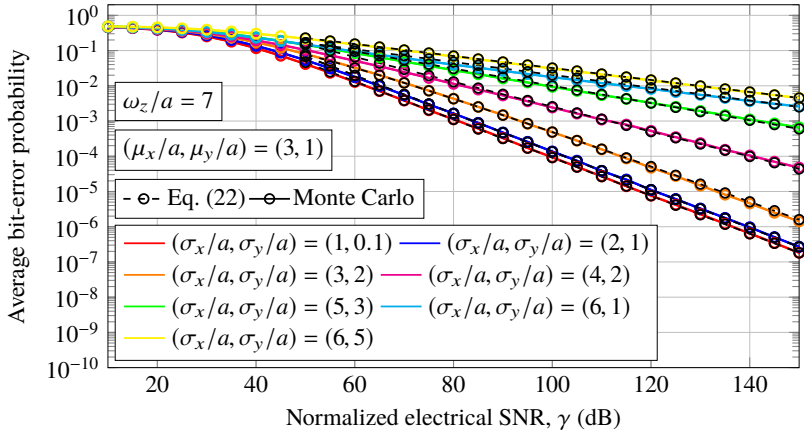

(b) Strong turbulence.

Fig. 3. BER performance over GG atmospheric turbulence and generalized misalignment fading channels, when different weather conditions (a) $C_n^2 = 1.7 \times 10^{-14}\ m^{-2/3}$ and (b) $C_n^2 = 8 \times 10^{-14}\ m^{-2/3}$ are assumed for a link distance of $d_{SD} = 3$ km.

Figs. 2 and 3. It is noteworthy to mention that the obtained results using the approximate PDF given in Eq. (16) provide quite a good match between the analytical and the respective Monte Carlo simulation results and, hence, not only a high accuracy of the proposed approximation is verified over the outage probability, but also over the asymptotic BER probability. Moreover, the accuracy of the proposed approximation not only is measured visually, but also quantitatively using curve-fitting metrics defined over a region of interest, as can be seen in appendix A. From the asymptotic BER, it is observed that this expression leads to a simple bound on the bit error probability that get tighter over a wider range of SNR as the turbulence strength increases.

Next, the impact of different jitters for the elevation and the horizontal displacement on the asymptotic BER probability of FSO systems is studied. As commented in the introduction section, one of the main contributions is to consider different jitters at the receiver. Hence, once the condition $\beta < \varphi_{\text{mod}}^2$ is satisfied and taking into account the asymptotic analysis carried out in section 4.2, we can obtain the disadvantage in decibels between considering and not considering pointing errors. Knowing that the impact of pointing errors in our analysis can be suppressed by

Optics EXPRESS

assuming $A_{\text{mod}} \to 1$ and $\varphi^2_{\text{mod}} \to \infty$, and considering the expression given in Eq. (22), the impact of the generalized pointing error effects translates into a coding gain disadvantage, D_{pe}[dB], relative to GG atmospheric turbulence without generalized misalignment fading given by

$$D_{pe}[dB] \triangleq (20/\beta)\log_{10}\left(\varphi^2_{\text{mod}}/\left(A_{\text{mod}}L\right)^{\beta}\left(\varphi^2_{\text{mod}}-\beta\right)\right). \tag{23}$$

Let us define the q parameter as the relation between σ_y/a and σ_x/a, where $q \in (0, 1]$, i.e., $\sigma_y/a = q\sigma_x/a$. Note that the lognormal-Rician pointing error model assumed in [11] is a special case when the q parameter is set to 1. For a better understanding of the impact of considering different jitters for the elevation and the horizontal displacement, the coding gain disadvantage, D_{pe}[dB] in Eq. (23), is depicted in Fig. 4 as a function of the q parameter when different normalized boresight error values are assumed. From Fig. 4, it can be deduced that the coding

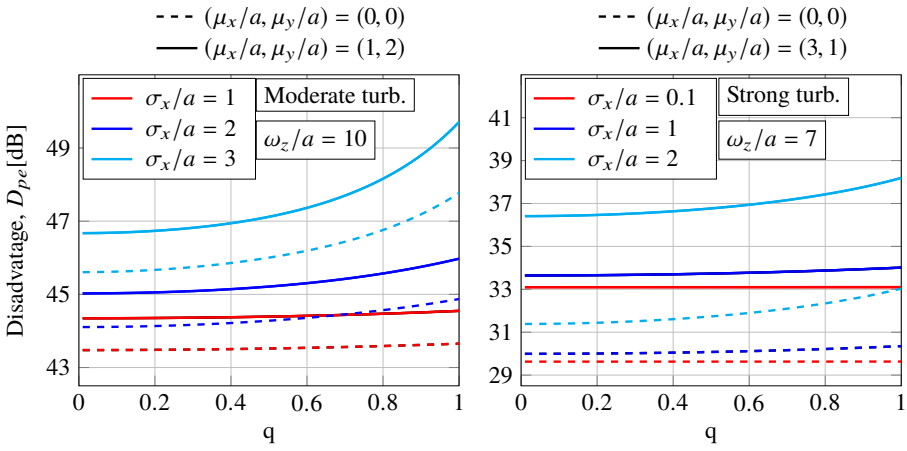

Fig. 4. Coding gain disadvantage, D_{pe}[dB], as a function of the q parameter for a link distance of $d_{SD} = 3$ km and different normalized boresight error values.

gain disadvantage increases as the normalized jitter σ_x/a increases. However, the coding gain disadvantage keeps practically constant when normalized jitter values much smaller than the normalized beam width are adopted. Equivalently, the same results and conclusions can be drawn when the q parameter is defined as $\sigma_x/a = q\sigma_y/a$. At the same time, the impact of nonzero boresight error is also studied in Fig. 5 as a function of the normalized horizontal boresight error when different normalized vertical boresight error values are assumed. As expected, the effect of nonzero boresight error can dramatically reduce the performance of FSO communication systems, increasing its effect as normalized jitter values increase. Equivalently, the same results and conclusions can be drawn when the impact of nonzero boresight is depicted as a function of the normalized vertical boresight error.

Finally, it should be commented that the adoption of the transmitter with accurate control of their beam width is especially important here in order to maximize the diversity order gain and minimize both outage and BER under different turbulence conditions. Therefore, a study of the required minimum normalized beam width is also included to guarantee that the relationship $\beta < \varphi^2_{\text{mod}}$ is always satisfied. We have to equate the corresponding expression of $\varphi^2_{\text{mod}} = \omega^2_{z_{eq}}/4\sigma^2_{\text{mod}}$ with the β parameter in order to know what the minimum value of normalized beam width makes the condition $\beta = \varphi^2_{\text{mod}}$ holds. Due to the fact that the corresponding expression of $\omega^2_{z_{eq}}$ appears to be cumbersome to use it, the equivalent beam width can be

Optics EXPRESS

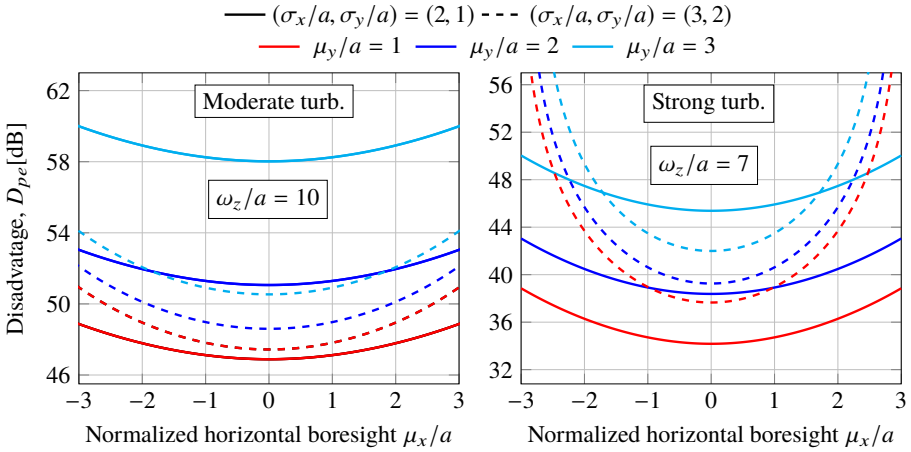

Fig. 5. Impact of nonzero boresight error as a function of the normalized horizontal boresight error μ_x/a for a link distance of $d_{SD} = 3$ km under different normalized vertical boresight error values of $\mu_y/a = \{1, 2, 3\}$.

approximated by a parabola with sufficient accuracy as follows

$$\omega_{z_{eq}}^2 = \frac{\omega_z^2\sqrt{\pi}\mathrm{erf}(v)}{2v\exp(-v^2)} \approx \omega_z^2 + \frac{3}{2\sqrt{2}}. \tag{24}$$

The above expression is quite simple and favors mathematical treatment. It can be deduced that the corresponding expression of φ_{mod}^2 is approximated as

$$\varphi_{\mathrm{mod}}^2 = \frac{\omega_{z_{eq}}^2}{4\sigma_{\mathrm{mod}}^2} \approx \frac{2\sqrt{2}\omega_z^2 + 3}{8\sqrt{2}\sigma_{\mathrm{mod}}^2}. \tag{25}$$

Now, we equate the expression in Eq. (25) with the β parameter and, after doing some easy algebraic manipulations, we obtain the required minimum normalized beam width to satisfy the relationship $\beta < \varphi_{\mathrm{mod}}^2$ as follows

$$\omega_{z_{min}}/a \approx 2^{-3/4}\left(2^{1/6}8\beta(3\mu_x^2\sigma_x^4 + 3\mu_y^2\sigma_y^4 + \sigma_x^6 + \sigma_y^6)^{1/3} - 3\right)^{1/2}. \tag{26}$$

The expression of $\omega_{z_{min}}/a$ in Eq. (26) is plotted in Fig. 6 as a function of the q parameter when different normalized boresight error values are assumed. It can be observed in Fig, 6 that the minimum value of the normalized beam width slowly increases as the the q parameter increases, being the worst case when the q parameter equals 1. It can be concluded that a greater severity of pointing error effects could be corrected with a increase in beam width in order to satisfy the condition $\beta < \varphi_{\mathrm{mod}}^2$, i.e., to achieve a much higher diversity order gain. It is noteworthy to mention that increasing the beam footprint also reduces the power incident on a fixed-size receiver and, hence, it is important to not significantly overestimate the necessary receiver beam size.

6. Conclusions

In this work, we have proposed quite an accurate approximation of the well-known Beckmann distribution, which is used to model generalized pointing errors. In this way, an approximate closed-form PDF for the composite GG atmospheric turbulence and generalized pointing errors

Optics EXPRESS

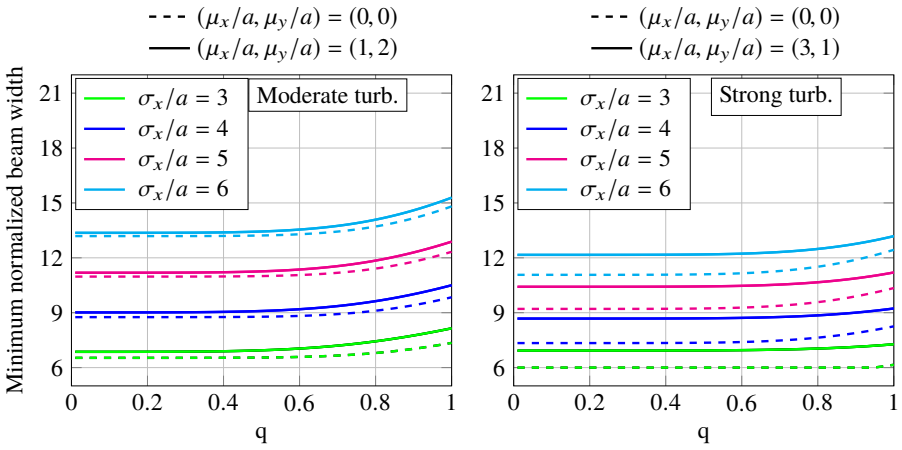

Fig. 6. Minimum normalized beam width as a function of the q parameter for a link distance of $d_{SD} = 3$ km and different normalized boresight error values.

is derived, which was used to evaluate the performance of terrestrial FSO links in terms of the outage probability and asymptotic BER. With the help of the proposed approximation, we have been able to throughly analyze two different FSO scenarios. On the one hand, we conclude that a much higher diversity order is achieved when atmospheric turbulence is the dominant effect in relation to generalized pointing errors, whose diversity gain is determined by the β parameter. On the other hand, the diversity order gain is decreased for larger amounts of misalignment, being this determined by the φ^2_{mod} parameter, which depends on the normalized beam width, normalized jitters for the elevation and the horizontal displacement as well as the nonzero boresight errors. Additionally, the proposed approximation have allowed us to analyze in a greater detail how some pointing error parameters such as beam width, different jitters as well as the effect of different nonzero boresight errors for each axis are able to modify the performance obtained for FSO communication systems. Moreover, due to the fact that FSO links require transmitters with accurate control of their beam width, this approximation was used to find the minimum normalized beam width that minimizes both outage probability and BER under different turbulence conditions. It was also demonstrated that the proposed approximation is very accurate over a wide range of SNR values.

Appendix A

In this appendix, we quantitatively measure the accuracy of the proposed approximation in a specific region of interest, in which the accuracy must be emphasized, taking as reference the illustrated FSO scenario in Fig. 2. Let $\hat{F}_{OP}(\cdot)$ denote the approximate outage probability expression derived in Eq. (19) and $F_{OP}(\cdot)$ the exact outage probability expression obtained by Monte Carlo simulations. Let $\gamma_1, \ldots, \gamma_N$ also denote N reference points in the region of interest. The accuracy metric for the outage probability is defined, as in [27], as

$$M_{OP} = \sum_{k=0}^{N} e_k \frac{| F_{OP}(\gamma_k) - \hat{F}_{OP}(\gamma_k) |}{F_{OP}(\gamma_k)}, \tag{27}$$

where e_k represents the relative error weight to emphasize different accuracies in tracking different reference points. Note that the following sum $\sum_{k=1}^{N} e_k = 1$ must be satisfied. In this work, the relatives error weights, e_k, are equal to $1/N$ for all k. At the same time, the region of interest is defined to be from $\gamma_1 = 20$ dB to $\gamma_N = 120$ dB, with the reference points spaced 5 dB

Optics EXPRESS

apart, i.e., $N = 21$. In this way, the accuracy metric, M_{OP}, is depicted in Fig. 7 as a function of the q parameter considering the same FSO scenario as in Fig. 2. It can be observed that a

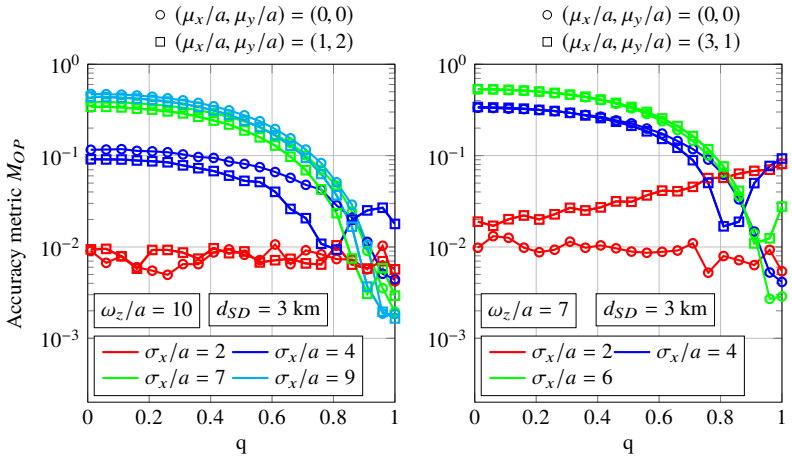

Fig. 7. Accuracy metric, M_{OP}, as a function of the q parameter for the outage probability when a source-destination link distance of $d_{SD} = 3$ km is assumed.

much higher achievable accuracy is obtained when small normalized jitter values are adopted, obtaining values of the order of 10^{-3}. Even when bigger normalized jitter values are assumed, an achievable accuracy of the order of 10^{-2} is obtained. In addition, the achievable accuracy is even much better as the q parameter increases. Analogously, it is depicted another accuracy metric in Fig. 8 as a practical example but considering another source-destination link distance of $d_{SD} = 5$ km in order to demonstrate the reliability of the proposed approximation in this work.

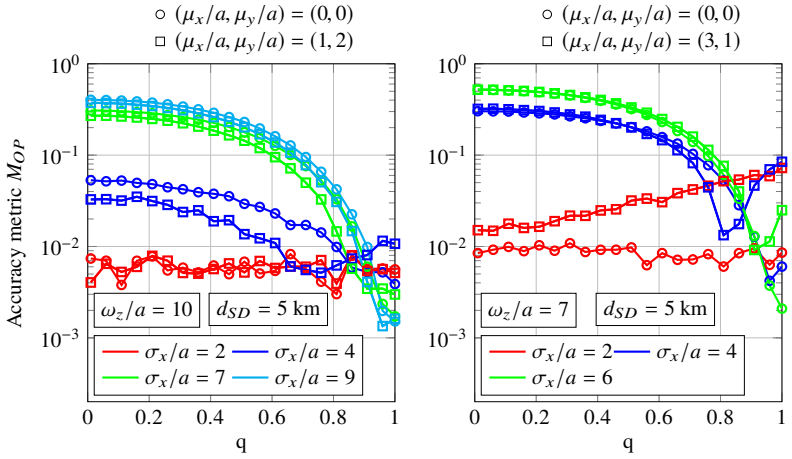

Fig. 8. Accuracy metric, M_{OP}, as a function of the q parameter for the outage probability when a source-destination link distance of $d_{SD} = 5$ km is assumed.

Funding

Junta de Andalucía (research group "Communications Engineering (TIC-0102)") and Universidad de Málaga.